Separation and Purification Technology 221 (2019) 83–92

Contents lists available at ScienceDirect

Separation and Purification Technology

journal homepage: www.elsevier.com/locate/seppur

Selective recovery of germanium from iron-rich solutions using a supported ionic liquid phase (SILP)

Stijn Van Roosendael[a], Joris Roosen[a], Dipanjan Banerjee[a,b], Koen Binnemans[a,*]

[a] KU Leuven, Department of Chemistry, Celestijnenlaan 200F, P.O. Box 2404, B-3001 Heverlee, Belgium
[b] Dutch-Belgian Beamline (DUBBLE), ESRF – The European Synchrotron, CS 40220, F-38043 Grenoble Cedex 9, France

ARTICLE INFO

Keywords:
Germanium
Goethite
Extraction chromatography
Ionic liquids
Metal recovery

ABSTRACT

A supported ionic liquid phase (SILP) was developed to selectively recover germanium from iron-rich aqueous solutions. The SILP was synthesised by impregnating Amberlite XAD-16N with Aliquat 336, a mixture of quaternary ammonium salts. Characterisation was performed using elemental analysis, infrared spectroscopy, specific surface area, porosity and density measurements. Adsorption was preceded by the addition of citrate anions to the iron-rich aqueous solutions, to form germanium(IV) citrate complexes, which were extracted to the ionic liquid layer of the SILP. The reaction kinetics and several adsorption parameters, including pH, anion concentration and adsorbent mass, were investigated using synthetic single-element germanium solutions. The coordination of germanium(IV) to the citrate ligands was elucidated using Extended X-ray Absorption Fine Structure (EXAFS). Subsequently, the optimal adsorption parameters were tested on a multi-element solution with elemental concentrations resembling those of a leachate of goethite residue from the zinc industry. A high selectivity for germanium over iron could be achieved. Finally, the stripping and the reusability of the SILP were studied. A germanium solution of 44 $mg{\cdot}L^{-1}$ was obtained with a germanium-over-iron mass ratio of 39. This corresponds to a selectivity factor equal to 34 400, demonstrating the high potential of the reported process.

1. Introduction

One of the key factors of resource efficiency is to treat 'waste' as a (secondary) source of raw materials [1]. Especially for the so-called "minor elements", which are not readily concentrated in ores, this is an imperative strategy. Often, these elements can be found in relatively high concentrations in certain waste streams, industrial residues in particular. Germanium is one of those elements [2]. Germanium is mainly used as a semiconductor in electronics and infrared optic industries, and as a polymerisation catalyst for the production of polyethylene terephthalate [3,4]. A few minerals exist with germanium as a main component, such as argyrodite, briartite, germanite, renierite and stottite, but these minerals are extremely rare and do not form rich ore deposits [4,5]. As a consequence, germanium is mainly obtained as a by-product of processing zinc ores [4,6–8]. On a global scale, only as little as 3% of all germanium contained in zinc concentrates is recovered [9]. Also certain coals contain significant concentrations of germanium, and their combustion results in germanium-rich ashes and flue dusts [7–9]. Since coals are often combusted at low temperatures to maximise germanium recovery, albeit without power generation, recovery of germanium from coal is not a sustainable process [10].

In the zinc processing industry, iron is removed from zinc sulphate solutions (obtained by leaching of zinc calcine with sulphuric acid) by precipitation as the iron minerals jarosite, goethite, paragoethite or hematite, depending on the type of process [11–13]. Goethite is an iron (III) oxyhydroxide, known to contain appreciable amounts of germanium; even an exceptionally high value of 5310 $mg{\cdot}kg^{-1}$ has been reported in the literature [14], although values of 100 to 229 $mg{\cdot}kg^{-1}$ are more common [15]. Currently, large amounts of goethite residue produced by the zinc-processing industry are landfilled, resulting in a loss of appreciable amounts of valuable metals, such as germanium [16,17]. Selective leaching of specific metals out of the goethite residue is problematic, since substantial amounts of impurities are leached as well. Co-leaching of iron is the main problem. To valorise the leachate, the present metals must be selectively separated so highly pure and valuable products are obtained. Traditionally, germanium is extracted from wastes by acidic oxidation leaching, followed by chlorination distillation to recover germanium as $GeCl_4$ [18]. However, pyrometallurgical processes like chlorination distillation or vacuum reduction, both technologies to recover germanium, are losing importance due to the formation of the volatile GeO and GeS compounds [5,18]. Other technologies are suited to recover germanium, including selective

* Corresponding author.
E-mail address: koen.binnemans@kuleuven.be (K. Binnemans).

https://doi.org/10.1016/j.seppur.2019.03.068
Received 5 December 2018; Received in revised form 10 February 2019; Accepted 23 March 2019
Available online 23 March 2019

extraction, ion exchange or ion flotation, many of them involving complexation with catechol [18]. Also precipitation by the addition of catechol or tannins can be used, with the latter being an expensive method due to the need to add oxalic acid as well [18]. In general, solvent extraction is a prevailing way in industry to separate metals in solution. In solvent extraction processes, metals are (selectively) extracted by extractants from an aqueous to an organic phase. With the purpose of reducing the viscosity of the organic phase and in this way enhancing extraction kinetics, organic diluents are quite often used [19]. As an alternative to molecular diluents in solvent extraction, *ionic liquids* have been introduced. These are a class of solvents which consist entirely of ions [19,20]. Attractive properties of ionic liquids include their negligible vapour pressure, low flammability, wide electrochemical window, high electrical conductivity and flexible tunability [21,22]. Important disadvantages arise from the high viscosity and the rather high price usually associated with ionic liquids [22]. As a consequence of the viscous or (partially) water-soluble organic phase, issues may arise from poor phase separation with the aqueous phase. These issues could be solved by coating a small layer of ionic liquid onto a solid support, thereby creating a *supported ionic liquid phase* (SILP). As a consequence, both the advantages of solvent extraction using ionic liquids (*i.e.*, high selectivity and tunability) and adsorption chromatography (*i.e.*, ease of phase separation and ability to treat large volumes of low-concentrated solutions) are combined [23]. The ionic liquid Aliquat 336 is interesting for this purpose as it is produced nowadays in multitonne scale and therefore commercially available and affordable [24]. Aliquat 336 is a commercial mixture of quaternary ammonium compounds with methyltrioctylammonium chloride as the main component. Aliquat 336 is an anion exchanger, which implies that metals are extracted in anionic form [25]. For germanium, many anionic complexes exist, so extraction to Aliquat 336 is feasible [2]. It has been reported that germanium(IV) citrate complexes can be quantitatively extracted by diluted Aliquat 336 from citric acid solutions [2,26] or even using Aliquat 336 coated on silica gel [27]. Moreover, citric acid is a complexing agent which is less harmful to the human health and is produced in a greener way compared to the widely used catechol for the recovery of germanium. A solvent-impregnated resin (SIR) system, based on the extractant di-(2-ethylhexyl)phosphoric acid (D2EHPA), has been studied to recover germanium, but very high acid concentrations ($[H^+] \geq 6\ mol{\cdot}L^{-1}$) were needed to obtain full germanium recovery [28,29].

In this paper, we studied the selective recovery of germanium from iron-rich solutions using citrate complexation and subsequent adsorption onto a SILP, consisting of Aliquat 336 impregnated onto a solid support, Amberlite XAD-16N. In addition to the synthesis and characterisation of the SILP, we report the parameter optimisation experiments performed on aqueous germanium-containing solutions, both single-element germanium solutions and synthetic mixtures simulating the composition of a real goethite leachate.

2. Experimental

2.1. Chemicals and materials

Amberlite XAD-16N (styrene-divinylbenzene copolymer, 20–60 mesh, 200 Å mean pore size), Aliquat® 336 (88.2–93.0% quaternary content), acetone (> 99.5%), iron powder (> 99%, fine), copper(II) sulphate pentahydrate (≥98.0%) and water-soluble (hexagonal) germanium(IV) oxide (≥99.99%) [30] were purchased from Sigma-Aldrich (Diegem, Belgium). Sulphuric acid (> 95% H_2SO_4), ethanol (99.99%) and sodium hydroxide (99.25%, pearls) were ordered from Fisher Scientific (Loughborough, United Kingdom). Magnesium sulphate (99.6%), iron(III) sulphate hydrate (≥21% Fe) and hydrochloric acid (36.5% HCl) were purchased from VWR Chemicals (Leuven, Belgium). Calcium sulphate dihydrate (> 99%), aluminium sulphate octadecahydrate (> 55% $Al_2(SO_4)_3$), ammonium chloride (> 99.8%), nitric acid (> 65% HNO_3) and 1000 $\mu g{\cdot}mL^{-1}$ ICP standard solutions were purchased from Chem-Lab nv (Zedelgem, Belgium). Anhydrous trisodium citrate (98%), manganese(II) sulphate monohydrate (> 99%), arsenic(III) chloride (99.5%) and zinc(II) sulphate monohydrate (99%) were purchased from Acros Organics (Geel, Belgium). Ethylenediaminetetraacetate disodium salt (Na_2-EDTA, 99.5%) was purchased from BDH laboratory supplies (Poole, England). Indium(III) sulphate (for synthesis, anhydrous) was purchased from Merck Schuchardt OHG (Hohenbrunn, Germany).

Amberlite® XAD-16N was purified before use (Section 2.3). All other chemicals were used as received, without further purification. All solutions were prepared using 18.2 MΩ·cm ultrapure water, produced by a Merck Milli-Q® Reference system.

2.2. Equipment and analysis

Fourier Transform Infrared (FTIR) spectra were recorded between 4000 and 400 cm^{-1} on a Bruker Vertex 70 spectrometer equipped with a platinum ATR module. CHN elemental analyses were performed using a Thermo Scientific Interscience Flash 2000 CHN(SO) elemental analyser. A Quantachrome Instruments NOVA 2000e volumetric adsorption analyser was used to record nitrogen adsorption-desorption isotherms at 77 K. From these, the specific surface area, and the pore volume and pore size distribution of the SILP material were calculated, based on the Brunauer-Emmet-Teller (BET) method and the Barrett-Joyner-Halenda (BJH) method, respectively. Prior to the measurements, the SILP material was degassed under vacuum for 20 h at 100 °C. The density of the SILP material was measured using an AccuPyc II 1340 pycnometer with a helium gas displacement system. A Büchi Rotavapor R-300 rotary evaporator was used to remove excess solvent from the ionic liquid phase or the SILP adsorbent particles. The metal composition of the aqueous solutions was measured using a Perkin Elmer Optima 8300 Inductively Coupled Plasma Optical Emission Spectrometer (ICP-OES) equipped with an axial (AX)/radial (RAD) dual plasma view, a GemTip Cross-Flow II nebuliser, a Scott double pass with inert Ryton® spray chamber and a demountable one-piece Hybrid XLT ceramic torch with a 2.0 mm internal diameter sapphire injector. Appropriate dilutions were made with 2 vol% nitric acid. Calibration curves, based on five standard solutions of known concentration (0.02, 0.10, 0.25, 1.00 and 10.00 $mg{\cdot}L^{-1}$), were constructed for all elements in the analysis. Scandium (5 $mg{\cdot}L^{-1}$) was added as an internal standard to each calibration and sample solution. Quality control samples were measured before and after measuring the sample series. All ICP-OES spectra were measured in triplicate. A Thermo Scientific MaxQ 2000 orbital shaker was used for all shaking experiments. A Mettler-Toledo pH-meter with a Hamilton Slimtrode pH electrode was used for pH measurements. To efficiently separate precipitates from solution, an Eppendorf 5804 centrifuge was used at 4000 rpm for 10 min. The technological flow sheet has been drawn using the web-based application draw.io (https://www.draw.io). All experiments were performed at room temperature.

The Extended X-ray Absorption Fine Structure (EXAFS) spectra of the germanium(IV) K edge (11,103 eV) were collected at the Dutch-Belgian Beamline (DUBBLE, BM26A) at the European Synchrotron Radiation Facility (ESRF) in Grenoble (France) by measuring a chloride solution containing 0.016 $mol{\cdot}L^{-1}$ Ge(IV) and 0.16 $mol{\cdot}L^{-1}$ trisodium citrate at pH 0.4 [31]. The energy of the X-ray beam was tuned by a double-crystal monochromator operating in fixed-exit mode using a silicon(1 1 1) crystal pair. The measurements were done in transmission mode using Ar/He gas filled ionisation chambers. A brass sample holder with Kapton® windows and a flexible polymeric spacer (VITON®) with a thickness of 2 mm was used as a sample holder. Standard procedures were used for pre-edge subtraction and data normalisation in order to isolate the EXAFS function (χ). The isolated EXAFS oscillations, accomplished by a smoothing spline as realised in the program Viper [32], were k^4 – weighted and Fourier transformed over the k-range from

2.25 to 10.75 $Å^{-1}$ using a Gaussian rounded end window function. The data were fitted using the ab initio code FEFF 7.0 [33], which was used to calculate the theoretical phase and amplitude functions subsequently used in the non-linear least-squares refinement of the experimental data. Fitting of the data with the model was performed in *R*-space. Standard errors on the data were estimated to be 5%. The amplitude reduction factor (S_0^2) was fixed for all fits at 0.93.

2.3. Synthesis of the SILP

Prior to impregnating the solid Amberlite XAD-16N particles with the Aliquat 336 ionic liquid, the Amberlite particles were purified. Sodium chloride salt, contained in Amberlite to retard bacterial growth, was washed out by adding ethanol (250 mL) to the Amberlite XAD-16N resin (200 g) and shaking for 2 h at 170 rpm. It was important to shake rather than to stir, since stirring would damage the beads. Subsequently, ethanol and dissolved salts were removed from the particles by filtration and the resin was washed twice with a small amount of ultrapure water and once with ethanol. Finally, ethanol was evaporated and the solid particles were equilibrated to air.

Physical impregnation was performed by combining Aliquat 336 (75 g) and the washed Amberlite XAD-16N (75 g) in acetone (375 mL). The mixture was shaken for 24 h, after which the acetone was removed using a rotary evaporator. To ensure a homogeneous SILP, the evaporation step was performed slowly. Then, the SILP was washed three times with ultrapure water (500 mL), each time separating the SILP from the aqueous solution by using a vacuum filtration system. Residual water was removed from the wet SILP in a vacuum oven at 45 °C for 48 h. Prior to characterisation and application, the SILP was equilibrated to air for another 24 h. The characteristic peaks of the FTIR spectrum of the Aliquat 336 SILP were: 3374 cm^{-1} (O—H stretch); 2954 cm^{-1}, 2923 cm^{-1} and 2854 cm^{-1} (C—H stretches); 1602 cm^{-1}, 1511 cm^{-1}, 1485 cm^{-1}, 1465 cm^{-1} and 1452 cm^{-1} (C=C aromatic ring stretches); 1377 cm^{-1} (C—H bend); 1117 cm^{-1} (C—N stretch tertiary amine); 989 cm^{-1}, 901 cm^{-1}, 830 cm^{-1}, 795 cm^{-1} and 709 cm^{-1} (aromatic C—H out-of-plane bends). The aromatic peaks arise from the Amberlite XAD-16N support material and the O—H stretch arises from the water content in Aliquat 336.

2.4. Adsorption parameters optimisation

Germanium single-element stock solutions (1132 $mg{\cdot}L^{-1}$ for sulphate and 1081 $mg{\cdot}L^{-1}$ for chloride medium) were made by dissolving a certain amount of GeO_2 in 0.1 $mol{\cdot}L^{-1}$ H_2SO_4 or 0.1 $mol{\cdot}L^{-1}$ HCl and adjusting the pH to 0.5 using 8 $mol{\cdot}L^{-1}$ H_2SO_4 or 8 $mol{\cdot}L^{-1}$ HCl, respectively. These solutions were then diluted 20 times after which the pH was adjusted to the appropriate value for the parameter optimisation using single-element solutions. Evidently, the exact germanium(IV) concentrations were dependent on the volume required for the pH adjustment. The multi-element stock solution was prepared by dissolving the sulphate metal salts in ultrapure water, except for arsenic, where $AsCl_3$ was used, and acidifying with concentrated H_2SO_4. Germanium was added to the mixture in the form of the germanium single-element stock solution.

Unless stated otherwise, adsorption experiments proceeded as follows. In closed glass vials, trisodium citrate 1 $mol{\cdot}L^{-1}$ (0.5 mL) was added together with SILP particles (500 mg) to a single-element germanium(IV) solution (10 mL, 59 $mg{\cdot}L^{-1}$, pH = 0.5, sulphate medium). The adsorption experiments were performed for 6 h by shaking the solutions at 175 rpm and room temperature in a mechanical shaker. After adsorption, the SILP particles were separated from the liquid by means of 0.45 μm syringe filters.

The optimised adsorption procedure was tested as well on a multi-element solution with metal concentrations resembling the concentrations of a typical goethite residue leachate. The multi-element solution had a pH equal to 0.5 and it contained iron(III) (23 216 $mg{\cdot}L^{-1}$), zinc (II) (13 318 $mg{\cdot}L^{-1}$), aluminium(III) (1 568 $mg{\cdot}L^{-1}$), copper(II) (940 $mg{\cdot}L^{-1}$), manganese(II) (683 $mg{\cdot}L^{-1}$), arsenic(III) (667 $mg{\cdot}L^{-1}$), calcium(II) (464 $mg{\cdot}L^{-1}$), magnesium(II) (381 $mg{\cdot}L^{-1}$), indium(III) (47 $mg{\cdot}L^{-1}$) and germanium(IV) (16 $mg{\cdot}L^{-1}$). To improve the selectivity, iron(III) was reduced to iron(II) by adding iron powder (600 mg) to the solution and shaking for 5 min. After separating the excess iron powder (and other solids) from the solution by using a paper filter, the same (optimised) adsorption procedure was applied on the multi-element solution.

Adsorption efficiencies (%*A*) were calculated by measuring the metal-ion composition of the aqueous solution before and after the adsorption experiment, using Eq. (1).

$$\%A = \frac{C_i - C_a}{C_i} \cdot 100 \tag{1}$$

where C_i is the initial metal concentration in solution and C_a is the metal concentration of the solution after adsorption. Since the added iron powder dissolved to a variable extent during each of the adsorption experiments, it was difficult to compare the iron adsorption amounts. Therefore, results for iron are generally not presented in the adsorption graphs where the multi-element solution was used.

2.5. Stripping parameters optimisation

Stripping tests were performed by first loading the SILP using the optimised adsorption procedure: adding iron powder (600 mg) to the multi-element solution (10 mL) of pH 0.5, reacting for 5 min, separating the solids from the aqueous phase, adding 1 $mol{\cdot}L^{-1}$ trisodium citrate (0.5 mL) and Aliquat 336 SILP (500 mg) and shaking for 6 h (see Section 3.3). Prior to stripping, the SILP was washed twice on top of the filter with ultrapure water (2 × 10 mL). Subsequently, a certain amount of the loaded SILP (between 50 mg and 500 mg) was contacted with a certain stripping solution for a certain time (between 1 min and 6 h). Solutions of different stripping agents (NH_4Cl, HCl, HNO_3 and Na_2-EDTA) in different concentrations were tested for their stripping potential. The stripping efficiencies (%*S*) were calculated by Eq. (2):

$$\%S = \frac{C_s \cdot V_s}{C_i \cdot V_i - C_a \cdot V_a} \cdot 100 \tag{2}$$

with C_s, C_i and C_a being the elemental concentration in the stripping solution, the initial solution and the solution after adsorption, respectively, and V_s, V_i and V_a being the volume of the stripping solution, the initial solution and the solution after adsorption, respectively. Up-concentration of the final product was performed by contacting the loaded SILP twice with a small volume (2 mL) of stripping solution for 1 h.

The selectivity of the recovery process (*S*) quantifies the preferential uptake of the target element (germanium) compared to the interfering matrix element(s) (mainly iron in this case) and is calculated using Eq. (3).

$$S = \frac{\left(\frac{C_{Ge}}{C_{Fe}}\right)_s}{\left(\frac{C_{Ge}}{C_{Fe}}\right)_i} \tag{3}$$

with $C_{Ge,s}$ and $C_{Fe,s}$ being the germanium and iron concentration in the stripping solution, respectively, and $C_{Ge,i}$ and $C_{Fe,i}$ being the germanium and iron concentration in the initial multi-element solution, respectively.

2.6. SILP reusability study

The reusability of the SILP was tested by performing five subsequent (optimised) adsorption – washing – stripping cycles on the multi-element solution. The experiments were performed with half the amount of SILP and half the amount of solution volumes compared to the

optimised procedure. The ratios between the different chemicals or materials remained the same. A washing step (shaking twice with 10 mL ultrapure water for 10 min) was included between the adsorption and the stripping cycle to remove any residual solution from the SILP.

3. Results and discussion

3.1. Synthesis of the SILP

When synthesising a SILP, the importance of the solid support should not be underestimated. Resins with a large specific surface area, with a pore size suitable for the application and which do not interact with the reaction medium are essential. Amberlite XAD-16N, a non-ionic macroreticular resin built up from styrene–divinylbenzene moieties, is an ideal candidate due to its inertness towards metal adsorption, its medium pore size of 20 nm and its large specific surface area of 800 $m^2 \cdot g^{-1}$ [34,35]. Evidently, the ionic liquid of which the SILP is composed, is of even higher importance to the SILP performance, since the metal (complex) exchange reactions occur at the aqueous/ionic-liquid interphase. Since Aliquat 336 is a well-known extractant for germanium(IV) and one of the cheapest commercially available ionic liquids, it was chosen for impregnation onto the solid Amberlite beads [2].

FTIR spectroscopy was used to prove the presence of quaternary ammonium groups on the SILP (Section 2.3). Further evidence for the successful impregnation of Aliquat 336 on the Amberlite resin was provided by CHN elemental analyses of the corresponding materials. The results can be seen in Table 1. The nitrogen content provides a clear indication that the Amberlite solid support was successfully impregnated with Aliquat 336. Since Aliquat 336 is a mixture of compounds, it was difficult to quantify the actual impregnated amount, but an estimation of the impregnation efficiency could be calculated by taking into account the molar ratio of octyl-to-decyl groups (2:1) in the Aliquat 336 mixture [36]. The percentage of ionic liquid impregnated onto the resin ($\%_{IL}$) was calculated by:

$$\%_{IL} = \frac{C_{N,SILP} - C_{N,support}}{C_{N,Aliquat336}} \cdot 100 = \frac{1.4wt\% - 0.1wt\%}{2.6wt\%} \cdot 100 = 50wt\% \quad (4)$$

where C_N refers to the nitrogen concentration in either the SILP, solid support (Amberlite XAD-16N) or ionic liquid (Aliquat 336).

Both the inner and outer surface of the porous SILP material were studied by nitrogen physisorption measurements. From the obtained adsorption-desorption isotherms, a subtle change from a hysteresis loop type IV for the washed Amberlite XAD-16N resin to a hysteresis loop type V for the Aliquat 336 SILP material could be recognised. This shows that monolayer-multilayer adsorption and capillary condensation take place, resulting in complete pore filling (*vide infra*), and weak adsorbate – adsorbent interactions occur [37]. To our interpretation, this suggests that the overall metal-uptake mechanism from the aqueous to the SILP phase is essentially driven by interaction with the impregnated ionic liquid. The total pore volume of the SILP material (0.29 $cm^3 \cdot g^{-1}$) is considerably smaller than the total pore volume of the washed solid support before impregnation (2.03 $cm^3 \cdot g^{-1}$). At the same time, the average pore radius of the SILP material (18.3 nm) is larger than of the washed solid support before impregnation (4.3 nm). The smaller total pore volume and increased average pore radius may be explained from the ionic liquid being deposited only on the surface of the solid support, therefore covering the smallest pores completely, but not the larger ones. From area-volume data derived from the nitrogen adsorption-desorption isotherms, it appeared that also the specific surface area of the solid support decreased drastically after impregnation with the ionic liquid: from 939 $m^2 \cdot g^{-1}$ for the washed Amberlite XAD-16N to 32 $m^2 \cdot g^{-1}$ for the SILP material. Thus, the surface of the support was largely covered with a layer of material with a less pronounced surface structure, the ionic liquid. The same observation has been described in related work on SILP materials, additionally indicating that the impregnation succeeded well [38].

The Aliquat 336 SILP has a density of 0.989 $g \cdot cm^{-3}$ at 25.6 °C. This value is an average of the reported densities of Amberlite XAD-16N (1.015–1.025 $g \cdot cm^{-3}$ [35]) and Aliquat 336 (0.8860 $g \cdot cm^{-3}$ [39]). This result provides even further evidence for the successful impregnation of the SILP.

Table 1
CHN elemental analysis results for pure Amberlite, Aliquat 336 and Aliquat 336 SILP.

	Pure Amberlite XAD-16N	Aliquat 336	Aliquat 336 SILP
C (wt%)	35.4 ± 1.0	71.3 ± 0.3	80.7 ± 0.2
H (wt%)	3.8 ± 1.2	12.7 ± 0.6	10.7 ± 0.1
N (wt%)	0.1 ± 0.1	2.6 ± 0.0	1.4 ± 0.0

3.2. Germanium(IV) citrate speciation

By adding citrate anions to the single-element (chloride) solution, germanium(IV) citrate complexes are formed, which can be extracted to the ionic liquid impregnated onto the solid support. Citrate had been selected as a complexing agent based on its germanium complexing potential [2,26], its biodegradability [40] and its relatively low price [41]. The speciation of the germanium(IV) citrate complex was studied by EXAFS spectroscopy. The EXAFS measurement was performed on a chloride solution containing 0.016 $mol \cdot L^{-1}$ Ge(IV) and 0.16 $mol \cdot L^{-1}$ trisodium citrate at pH 0.4. The EXAFS spectrum and the fitted curve of the germanium(IV) citrate complex is shown in Fig. 1 and the Fourier transform (FT) function with the corresponding fitted curve is shown in Fig. 2.

An excellent fit of the first peak in the FT of the EXAFS function of the germanium(IV) citrate complex could be obtained using a GeO_6 octahedral model. The number of surrounding oxygen atoms was found to be 6.0 and the average bond length between germanium and oxygen was determined to be 1.889 Å from the fit. This is in agreement with crystal structures of octahedral germanium(IV) complexes with only oxygen atoms in the first coordination sphere [42–44]. No chloride atom was found, which should be located around 2.29 Å in an octahedral germanium(IV) complex [45].

There is a general trend in the germanium–carbon path length depending on the ring size of the multidentate polycarboxylate or similar ligand. Either a Ge–C path length of approximately 2.7 Å is found for five-membered rings, containing one carboxylate function and the alcohol function of a polydentate ligand, or a Ge–C path length of approximately 2.9 Å is found in case of a six-membered ring with two carboxylate functions coordinating the germanium(IV) center [42,43].

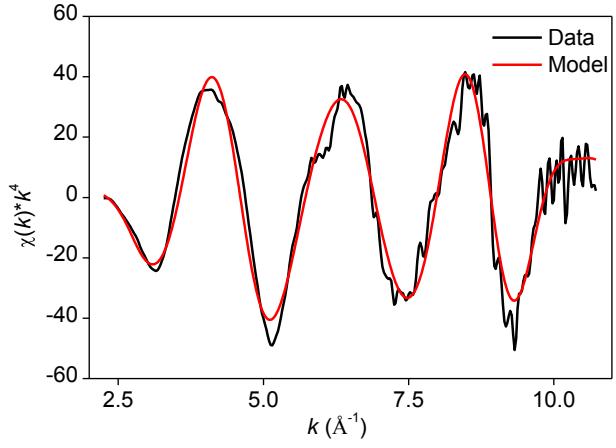

Fig. 1. EXAFS spectrum of the germanium(IV) citrate complex.

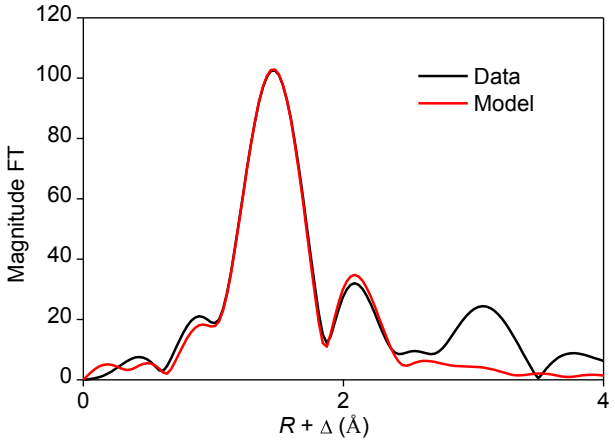

Fig. 2. Fourier transform of the EXAFS function of the germanium(IV) citrate complex.

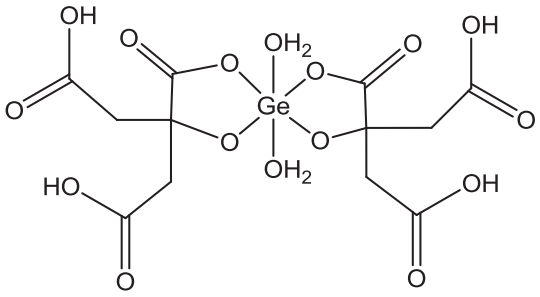

Fig. 3. Chemical structure of the germanium(IV) citrate complex.

The second peak in the FT of the germanium(IV)-citrate complex (Fig. 2) could be fitted by a Ge–C single scattering path with a path length of 2.667 Å. The coordination number and Debye–Waller factor found for this path are 2.4 and 0.002 $Å^2$, respectively. The very low Debye–Waller factor and the fact that the coordination number and Debye–Waller factor are strongly correlated suggest that the degeneracy of this path is probably higher than 2.4. A degeneracy of 4.2 was found when constraining the Debye–Waller factor to a reasonable value of 0.007 $Å^2$. A degeneracy of 6.0 was found if the Debye–Waller factor was constrained to a value of 0.015 $Å^2$. The latter value is very high for this kind of path suggesting that a Ge–C degeneracy of 4.2 is more likely to be present. No peak was observed and no carbon could be fitted at a Ge–C path length of 2.9 Å, supporting the hypothesis of citrate ligands forming five-membered rings with germanium(IV).

The third peak in the FT (Fig. 2) can be attributed to the scattering paths involving the nearest carbon atoms in the other carboxylic acid arms of the citrate ligand. This peak was not fitted because of the contribution of several unknown paths. The non-fitting of this peak also leads to a non-perfect fitting of the EXAFS function (Fig. 1). Nonetheless, EXAFS analysis suggests that germanium(IV) is coordinated by two bidentate citrate ligands. The citrate ligands are binding the germanium(IV) center by one of their carboxylic acid groups and by their alcohol functionality. The remaining two coordination sites are presumably occupied by water molecules. This conclusion is in agreement with literature data [46]. The chemical structure of the defined germanium(IV) citrate complex is shown in Fig. 3.

3.3. Adsorption parameters optimisation

Prior to testing the more relevant multi-element solutions, the performance of the SILP was tested on single-element germanium solutions. This way, the uptake of germanium could be assessed without other elements influencing the adsorption mechanism. First, the

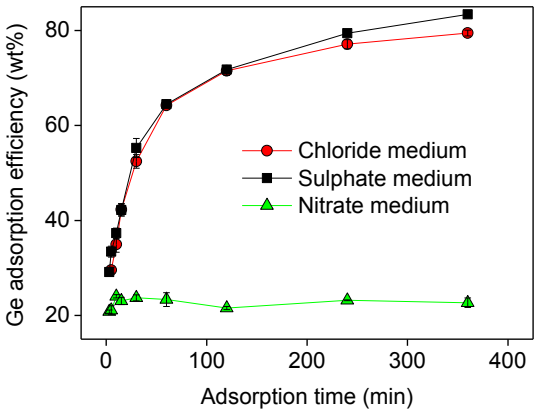

Fig. 4. SILP adsorption kinetics from single-element germanium solutions consisting of different anionic media (10 mL solution, 54 $mg{\cdot}L^{-1}$ Ge(IV) (chloride), 59 $mg{\cdot}L^{-1}$ Ge(IV) (sulphate), 58 $mg{\cdot}L^{-1}$ Ge(IV) (nitrate), 0.05 $mol{\cdot}L^{-1}$ trisodium citrate, 100 mg of SILP, 1–360 min adsorption, pH 0.75).

adsorption kinetics were investigated by adding 100 mg of SILP to 10 mL solution (pH = 0.75) containing 54–59 $mg{\cdot}L^{-1}$ germanium(IV) (depending on the medium) and 0.05 $mol{\cdot}L^{-1}$ trisodium citrate and varying the time during which the mixture was shaken. From Fig. 4, it can be seen that germanium can be adsorbed from both chloride and sulphate medium, but not from nitrate medium. The position of the chloride anion in the Hofmeister series is more to the right than the sulphate or hydrogen sulphate anions and therefore, generally, little anion exchange occurs between the hydrophobic chloride SILP and the sulphate containing aqueous solution [47,48]. If there would be some anion exchange during the adsorption step, then the ionic liquid may be regenerated during the HCl stripping step (*vide infra*). However, anion exchange between the nitrate aqueous solution and the chloride SILP will occur due to the higher hydrophobicity of the nitrate anion, which in turn leads to an inefficient anion exchange reaction with the germanium complex and therefore low extraction efficiencies. An additional observation about the performed experiment is that the adsorption kinetics are rather slow. As can be seen in Fig. 4, after 6 h of adsorption, still no plateau value was reached. However, it was expected that the benefit of reaching equilibrium, and therefore recovering the maximum amount of germanium from solution, did not compensate for the extra time needed to reach this equilibrium. Therefore, it was decided that an adsorption time of 6 h was sufficientl.

Since sulphuric acid is the most relevant acid (less expensive than nitric acid and less corrosive than hydrochloric acid), only sulphate solutions were considered further on. Although the EXAFS measurements were performed on the chloride system, it is expected that the speciation of the germanium(IV) citrate complex is similar in the sulphate system for two reasons: (1) no chloride atoms were detected in the first coordination sphere in the EXAFS study and (2) a very similar adsorption behaviour was observed from both chloride and sulphate systems, as can be seen in Fig. 4.

Next, the influence of pH on the germanium adsorption efficiency was studied. Given that the germanium adsorption efficiency in the previous experiment was only 83.4% after 6 h of adsorption, the amount of SILP was increased (to 250 mg) to obtain higher adsorption efficiencies. Due to the very low solubility product constant of $Ge(OH)_4$ ($K_{sp} = 2.39 \cdot 10^{-45}$) [49], hydrolysis should not be underestimated. Therefore it was considered important to measure a blank (without adding SILP) at each pH value as well. As can be observed in Fig. 5, an increase in pH results in an increase in germanium adsorption efficiency. This is as expected, since lower pH values generate more protonated citrate molecules, which are thus less available for complexation with germanium(IV). Also the co-extraction of citrate to Aliquat 336 (impregnated on the SILP) is enhanced at lower pH values [50]. It

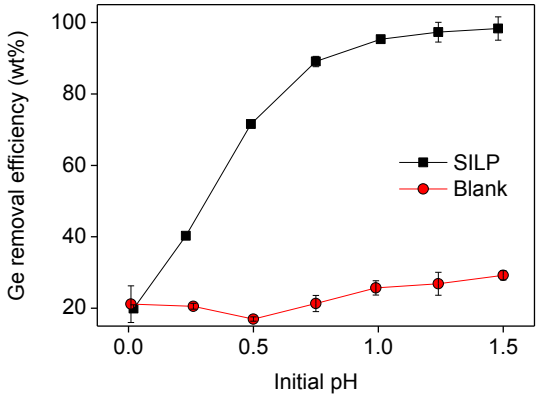

Fig. 5. pH influence on the germanium removal (adsorption) efficiency (10 mL solution, 59 mg·L^{-1} Ge(IV) (sulphate), 0.05 mol·L^{-1} trisodium citrate, 250 mg of SILP, 6 h adsorption, pH 0–1.5).

is also clear that even at very low pH values, already 20% of germanium was removed from solution, even from the blank. At pH values higher than 0.75, the increasing amount of removed germanium can be explained by hydrolysis-precipitation. In order to obtain reasonable germanium adsorption efficiencies and minimal amounts of blank removal, a pH value of 0.75 was used in the following single-element solution experiments.

The next two parameters studied (simultaneously) on the single-element germanium solutions were the influence of the citrate concentration and the influence of the SILP mass on the germanium adsorption efficiency. The results are shown in Fig. 6. As can be seen, there is a sharp increase in germanium adsorption efficiency with increasing citrate concentration up to 0.05 mol·L^{-1}, after which the germanium adsorption efficiency steadily decreases again. The increase in germanium adsorption efficiency can be explained by the fact that a certain amount of citrate anions is needed to form the germanium citrate complexes, resulting in an increase in germanium adsorption efficiency with higher citrate concentration. The reason to why the germanium adsorption efficiency is decreasing at even higher citrate concentrations, is less straightforward. The most viable explanation is that citrate anions are also adsorbed to the SILP, resulting in a competitive adsorption between the germanium(IV) citrate complexes and the excess citrate anions [50,51]. However, two other hypotheses could be true. Hypothesis 1: At too high citrate concentration, the citrate anions might no longer bind to germanium(IV) in a bidentate way, but rather in a monodentate way, resulting in quite bulky complexes. These bulky complexes must be compensated by a larger number of Aliquat 336 molecules, so less germanium citrate complexes could be extracted to the same amount of Aliquat 336, thus leading to a decrease in germanium adsorption efficiency. This explanation is closely related to the second hypothesis. Hypothesis 2: When citrate would bind in a monodentate way to germanium(IV), the bulky complexes might not be able to penetrate through the pores of the SILP. When more of these bulky complexes would be formed, less complexes would be adsorbed to the SILP. It has already been reported in the literature that higher citrate concentrations could result in the formation of monodentate uranium (VI) citrate complexes [52], but for germanium(IV) citrate complexes this has not been reported yet.

Either way, the optimal citrate concentration was set at 0.05 mol·L^{-1} for these germanium concentration levels. Moreover, it can be seen that, in order to achieve high germanium adsorption efficiencies, a lot of SILP was needed: 500 mg of SILP appeared to be required to obtain a fairly high (almost quantitative) germanium adsorption efficiency. This corresponds to a concentration of 1.01 g germanium per kg of SILP, which is significantly lower than the germanium concentration on the SILP when less SILP would be used. However, it is preferred to obtain a high germanium adsorption efficiency compared to using the full potential of the SILP (but hereby also decreasing the total germanium adsorption efficiency).

After studying all parameters on single-element germanium solutions, the adsorption of germanium was studied from multi-element solutions. The influence of the pH on the adsorption characteristics was studied by using the previously mentioned optimal parameters, being an adsorption duration of 6 h, a citrate concentration of 0.05 mol·L^{-1} and a SILP mass of 500 mg. Since a lot of iron(III) is present in the multi-element solution, which forms stable citrate complexes and would thus consume all the citrate anions and saturate the SILP with unwanted iron(III) complexes, iron(III) had to be removed from solution prior to the addition of citrate anions. Selective hydrolysis-precipitation of iron is not possible since germanium(IV) co-precipitates at pH values at which full iron(III) hydrolysis precipitation cannot yet be achieved, as can also be seen later in the manuscript (Fig. 7). Also large amounts of chemicals would be necessary to first increase and in a later stage decrease the pH. Therefore, iron(III) was reduced to iron(II) by the addition of iron powder since iron (II) citrate complexes have a significantly lower stability constant (log K = 4.8) compared to the iron(III) citrate complexes (log K = 11.2) [53]. The reduction was done by exploiting the following comproportionation reaction with iron powder:

$$2Fe^{3+} + Fe^{0} \rightarrow 3\ Fe^{2+} \quad (5)$$

Since iron(II) can reoxidise to iron(III) by contact with oxygen dissolved from the air, an excess of iron powder (600 mg for 10 mL solution in this case) is required. Of course, the excess can be recovered and reused in a later stage.

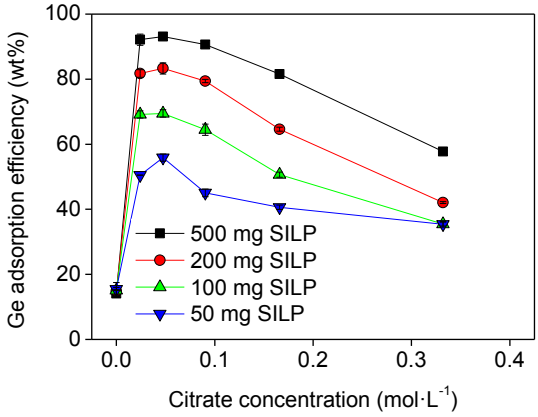

Fig. 6. Influence of the citrate concentration and the SILP mass on the germanium adsorption efficiency (10 mL solution, 59 mg·L^{-1} Ge(IV) (sulphate), 0–0.33 mol·L^{-1} trisodium citrate, 50–500 mg of SILP, 6 h adsorption, pH 0.75).

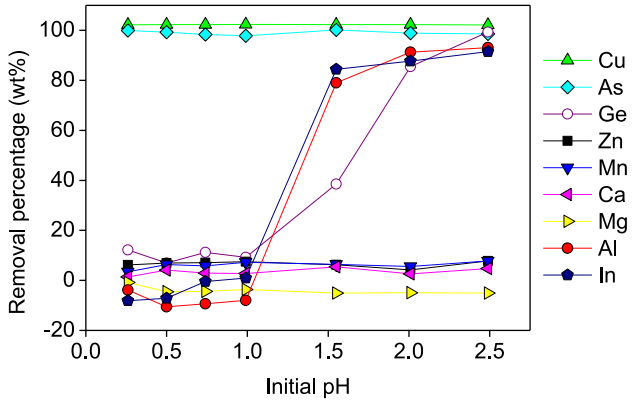

Fig. 7. pH influence on the metal removal percentage for a multi-element solution (=blank measurement) (10 mL solution, 17 mg·L^{-1} Ge(IV) (sulphate), 0.05 mol·L^{-1} trisodium citrate, 0 mg of SILP, 6 h adsorption, pH 0.25–2.5).

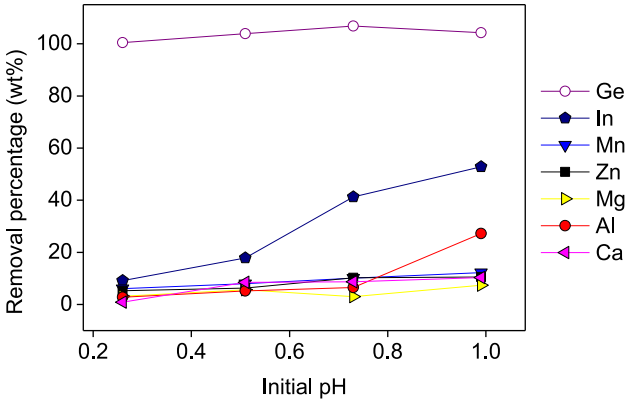

Fig. 8. pH influence on the metal removal percentage using the SILP for a multi-element solution (10 mL solution, 17 mg·L^{-1} Ge(IV) (sulphate), 0.05 mol·L^{-1} trisodium citrate, 500 mg of SILP, 6 h adsorption, pH 0.25–1).

Results of the multi-element pH experiment are shown in Figs. 7 and 8, corresponding to the blank measurement and the measurement using the SILP, respectively. In order not to overcomplicate the figures, standard deviations are not added to these two figures. Iron is not shown in the figures since extra iron was added to the solution (as iron powder partially reacting to iron(II)), thus complicating calculation of the removal percentage. Apart from iron reduction, addition of iron powder to the multi-element solution had the additional effect of completely removing copper(II) and arsenic(III) from solution by reduction to the metallic state. This is an advantage, as copper(II) would form stable extractable citrate complexes as well, in addition to germanium(IV). Since arsenic(III) is toxic and forms a potential environmental hazard, it is beneficial to remove it from solution in order to obtain a concentrated product for controlled waste disposal. Also titanium(IV), which was not present in the multi-element solution, albeit possibly present in goethite residue, could be separated as a solid by addition of iron powder. For clarity reasons, the removed elements are not presented in Fig. 8. From Fig. 7, it is clear that a pH of 1 or less is necessary to avoid precipitation of metals, this way causing germanium co-precipitation. In Fig. 8, the pH range was therefore limited to the most interesting values, from pH 0.25 to 1.00. It is also clear from Fig. 8 that germanium can be completely adsorbed to the SILP in a highly selective way (i.e. with minimal adsorbent contamination by other elements). At pH values above 0.5, other elements such as indium(III) and aluminium(III) get adsorbed too. Therefore, it was decided to keep the pH at 0.5 (or lower) when using multi-element solutions. For further experiments, iron powder was added to the multi-element solution and after reacting for 5 min, the solid precipitate was separated from the aqueous (purified) solution.

After recovering germanium(IV) from the multi-element solution, it must be stripped from the solid adsorbent to an aqueous phase. In Table 2, a screening study is presented where three types of stripping agents (10 mL) were assessed in different concentrations: NH_4Cl as source of chloride anions, HNO_3 as strong acid – simultaneously supplying nitrate counter anions (from which extraction was already shown to be poor, see Fig. 4), and Na_2-EDTA as a commonly used complexing agent. Prior to stripping, the SILP was washed twice with ultrapure water (2 × 10 mL). A first thing to notice is that both the NH_4Cl solutions with a high chloride content and HNO_3 solutions were able to strip germanium in an efficient way. Iron and zinc seemed to be the main impurities in the respective stripping solutions. However, both metals can be selectively removed from the SILP by stripping with a Na_2-EDTA solution, without affecting the loaded germanium(IV) ions. As such, this step could be considered as a scrubbing step prior to stripping of germanium(IV). Loosely bound impurities can be removed by a thorough washing procedure. Then, iron and zinc can be scrubbed using a 0.05 mol·L^{-1} Na_2-EDTA solution. Finally, stripping of pure germanium can be achieved by either NH_4Cl or HNO_3 solutions. Given that the SILP is composed of chloride anions, the best option would be to use a (1 mol·L^{-1}) chloride stripping solution, thus avoiding anion exchange between the aqueous phase and the SILP, which would lead to the need of regenerating the SILP.

Table 2
Elemental concentration of the loaded stripping solutions.

Stripping solution	Elemental concentration (mg·L^{-1})									
	Fe	Zn	Al	Cu	Mn	As	Ca	Mg	In	Ge
0.25 mol·L^{-1} NH_4Cl	298	18	10	0	4	1	4	2	1	3
0.5 mol·L^{-1} NH_4Cl	307	6	11	0	4	1	5	2	1	10
1 mol·L^{-1} NH_4Cl	306	2	11	0	4	2	4	2	0	**15**
2 mol·L^{-1} NH_4Cl	302	1	11	0	4	1	4	2	0	**16**
4 mol·L^{-1} NH_4Cl	279	2	10	0	4	2	4	2	0	**16**
0.1 mol·L^{-1} HNO_3	322	275	10	0	5	1	4	2	1	**14**
0.25 mol·L^{-1} HNO_3	325	274	11	0	5	2	4	2	1	**16**
0.5 mol·L^{-1} HNO_3	314	275	10	0	4	1	4	2	1	**17**
1 mol·L^{-1} HNO_3	316	272	10	0	4	1	5	2	1	**16**
2 mol·L^{-1} HNO_3	325	279	11	0	5	1	5	2	1	**17**
0.05 mol·L^{-1} Na_2-EDTA	**292**	**217**	7	0	4	2	4	2	1	0
0.1 mol·L^{-1} Na_2-EDTA	**282**	**213**	7	0	4	1	4	2	1	0
0.25 mol·L^{-1} Na_2-EDTA	**302**	**224**	8	0	4	1	5	3	1	0
1 mol·L^{-1} Na_2-EDTA	**244**	**205**	7	0	3	1	5	2	1	0

Next, the combined scrubbing and stripping approach was attempted. After scrubbing the loaded SILP with a 0.05 mol·L^{-1} Na_2-EDTA solution, HCl was used as stripping agent instead of NH_4Cl, in order to ensure that the pH was low enough to keep germanium dissolved in the aqueous phase. The washing procedure, applied both after the adsorption and the scrubbing step, was altered by shaking the SILP three times for 10 min using 10 mL of ultrapure water each time. Additionally, it would be interesting to concentrate the germanium(IV) solution. Consequently, also the used volume of stripping solution was an important parameter and was therefore considered as well. Not only single stripping steps were studied, but two tests were performed as well where the same amount of stripping solution was used twice. All results are shown in Table 3, where the first data row refers to the scrubbing step. Logically, if larger stripping solution volumes are used, the elemental concentrations in the stripping solutions are lower. Based on the total amount of germanium stripped in combination with the ability to concentrate, stripping two subsequent times using 2 mL of 1 mol·L^{-1} HCl solution each time (the last option in the table) was concluded to be the better option. After the first stripping step, 81% of the total amount of germanium(IV) loaded on the SILP was already stripped. The second stripping step increased the total stripping efficiency to 100%.

Table 3
Influence of the HCl concentration and the volume of HCl solution on the metal composition of the stripping solution.

Stripping solution volume and concentration	Elemental concentration (mg·L^{-1})									
	Fe	Zn	Al	Cu	Mn	As	Ca	Mg	In	Ge
10 mL 0.05 mol·L^{-1} Na_2-EDTA	59	42	1	1	1	1	5	0	0	0
10 mL 0.1 mol·L^{-1} HCl	4	4	1	0	0	0	1	0	0	8
10 mL 1 mol·L^{-1} HCl	3	0	1	0	0	0	1	0	0	19
10 mL 4 mol·L^{-1} HCl	0	5	1	0	0	0	1	0	0	18
5 mL 1 mol·L^{-1} HCl	4	0	2	0	0	0	1	0	0	35
5 mL 2 mol·L^{-1} HCl	1	4	3	0	0	0	2	0	0	36
2 mL 1 mol·L^{-1} HCl	8	0	5	0	0	0	2	0	0	67
2 × 5 mL 1 mol·L^{-1} HCl*	2	0	1	0	0	0	1	0	0	19
2 × 2 mL 1 mol·L^{-1} HCl*	5	1	3	0	0	0	2	0	0	44

* The data of the two-step stripping experiments (two last rows) relate to the average concentration values of the two stripping solutions combined.

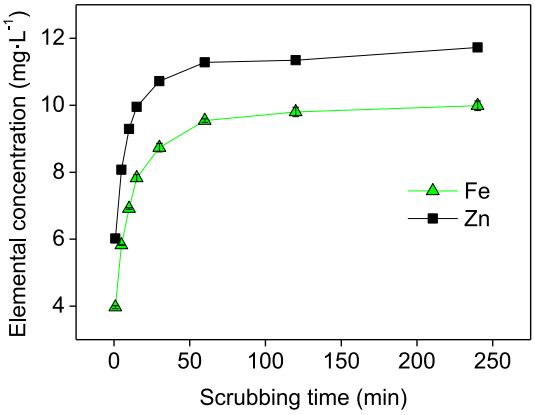

Fig. 9. Influence of the scrubbing time on the elemental concentration of the scrubbing solution (optimal adsorption parameters, 10 mL of EDTA solution (0.05 mol·L^{-1}), 1–240 min scrubbing time).

Lastly, the scrubbing and stripping kinetics were studied using a further optimised washing procedure and scrubbing/stripping solutions, although only one stripping cycle using 2 mL of 1 mol·L^{-1} HCl solution was performed instead of the double stripping cycle. The results are shown in Figs. 9 and 10, respectively. A conclusion was made that for both the scrubbing and the stripping step a duration of 1 h is required. Since the optimal stripping procedure consists of two subsequent stripping cycles, the total stripping time is 2 h. The concentration of iron and zinc in the scrubbing solution are lower compared to the values in (the first row of) Table 3 as a result of the improved washing procedure. This also results in lower amounts of iron in the final stripping solution. The contaminants present in the stripping solution are iron, aluminium and calcium, all of them in a concentration of only 1 mg·L^{-1}.

When applying the optimal adsorption – scrubbing – stripping procedure on the multi-element solution (with washing steps in between), a germanium solution of 44 mg·L^{-1} was obtained (corresponding to complete germanium recovery) with a germanium-over-iron mass ratio of 39 and a selectivity factor as high as 34 400. Therefore, this method is extremely selective for germanium, especially compared to the large amount of iron present in the original solution.

3.4. SILP reusability

The reusability of the SILP was studied by performing five subsequent adsorption – scrubbing – stripping cycles on the multi-element

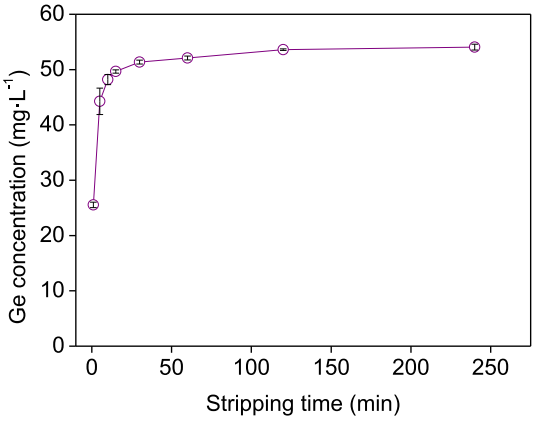

Fig. 10. Influence of the stripping time on the germanium concentration in the stripping solution (optimal adsorption parameters, 10 mL of EDTA scrubbing solution (0.05 mol·L^{-1}), 240 min scrubbing time, 2 mL stripping solution, 1–240 min stripping time).

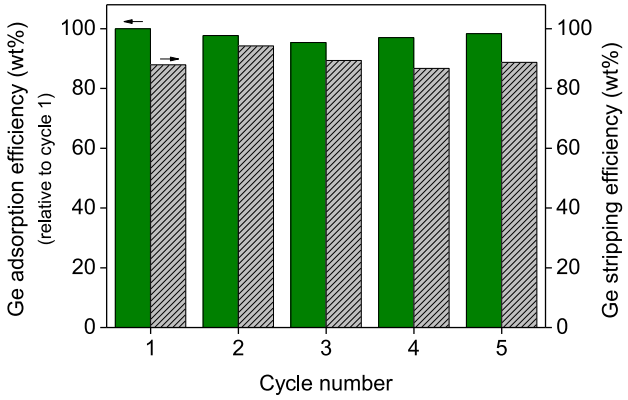

Fig. 11. Germanium adsorption efficiencies (full bars, left Y–axis, relative to cycle 1) and stripping efficiencies (dashed bars, right Y-axis) for five subsequent adsorption – scrubbing – stripping cycles, using the optimal parameter setup.

stock solution. In case there would be some minor anion exchange during the adsorption step, the SILP would be regenerated during the stripping step using HCl, leading to a steady adsorption efficiency in the next cycle. As can be seen in Fig. 11, the germanium adsorption efficiency remains rather constant during all cycles. Also the stripping efficiencies remained more or less constant, with the exception of the stripping efficiency obtained after the stripping step in the second cycle, which is a bit elevated compared to the other cycles. Compared to the previous experiments, where 100% of the germanium was stripped, only 89% of germanium was stripped (on average) in the reusability experiment. This is the result of using a really small stripping solution volume (1 mL instead of 2 mL) but in the same glass vial, which results in a less opportune contact between the stripping solution and the SILP. The variation on the stripping efficiencies was predicted to vary more compared to the adsorption efficiencies since more manipulations are in between the addition of the stock solution and the stripping step itself. It can be concluded that the developed method can be used multiple times without decrease in performance.

A flowsheet for the recovery of germanium from a dilute germanium – iron solution, such as a goethite type of leachate, is presented in Fig. 12. The proposed flowsheet is based on a batch process. If this flowsheet would be transformed into a flowsheet for a column setup, some process steps could be eliminated. If, for instance, two columns would be placed in series, with the first column containing solid iron particles (to reduce iron(III) to iron(II)) and the second column containing the SILP, the 'filtration' steps would no longer be necessary. The only necessity is a regular refill of the first column with iron scrap. Moreover, the adsorption, washing, scrubbing and stripping steps may seem as separate steps within the process, but in practice, there is no need to transfer the SILP particles from one column to another.

4. Conclusions

A flowsheet is proposed for the selective recovery of germanium from iron-rich solutions. The developed system, based on SILP technology, appeared to be highly selective for germanium. First, an Aliquat 336 SILP was prepared by physical impregnation of Amberlite XAD-16N with the ionic liquid Aliquat 336. The adsorption procedure was fully optimised and quantitative recovery was reached for 10 mL of a single-element germanium solution (59 mg·L^{-1}) by adding 0.5 mL of citrate solution (1 mol·L^{-1}) and 500 mg of SILP, and contacting for 6 h. After adsorption and washing, a scrubbing step using an EDTA solution (0.05 mol·L^{-1}) showed to be efficient in removing small amounts of iron and zinc impurities. After washing the SILP again to remove the excess of EDTA solution, the SILP was stripped using a two-step stripping procedure, each stripping step using 2 mL of a 1 mol·L^{-1} HCl solution and lasting for 1 h each. A concentrated germanium solution of

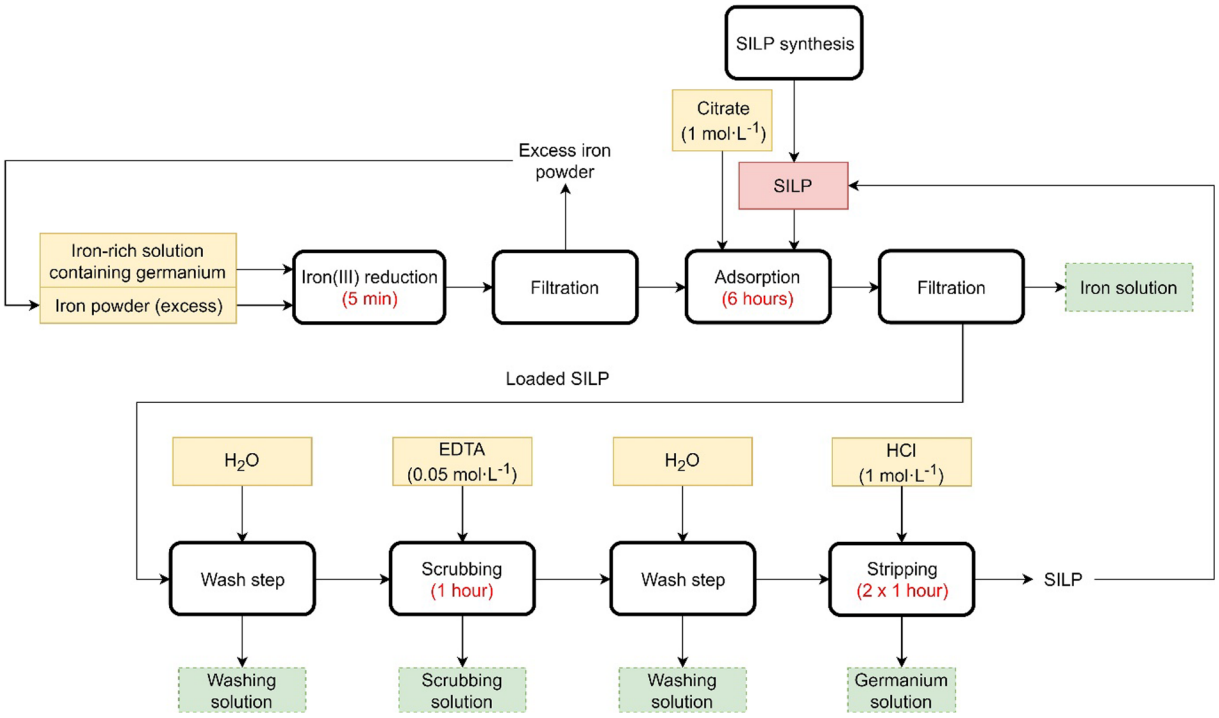

Fig. 12. Proposed flowsheet for the recovery of germanium from an iron-rich matrix solution using an Aliquat 336 SILP in batch mode (2-column figure).

44 $mg{\cdot}L^{-1}$ was obtained (corresponding to full germanium recovery), with a germanium-over-iron mass ratio of 39 and a selectivity factor equal to 34 400, starting from a multi-element solution resembling an actual leachate of goethite residue. Moreover, the SILP system appeared to be reusable in multiple cycles without losses in terms of adsorption or stripping efficiency and without the need to regenerate the SILP adsorbent. In conclusion, the developed flowsheet has a high potential for the selective recovery of germanium (present in low concentrations) from iron-rich solutions, such as acidic leachates from goethite residue of the zinc industry.

Conflicts of interest

There are no conflicts of interest to declare.

Acknowledgements

This work was supported by the European Union's Horizon 2020 research and innovation programme: Metal Recovery from Low-Grade Ores and Wastes Plus (METGROW +) [grant number 690088]. Project website: https://metgrowplus.eu. The FWO Flanders is acknowledged for supporting the DUBBLE beamline at the ESRF (France). The authors would like to thank Dr. Tom Vander Hoogerstraete for assistance in EXAFS measurements and data analysis, Dirk Henot for performing the CHN analysis, Gerrit Van Haele for performing the BET analysis and Dr. Mercedes Regadío for scientific guidance during preliminary experiments.

References

[1] V. Prieto-Sandoval, C. Jaca, M. Ormazabal, Towards a consensus on the circular economy, J. Clean. Prod. 179 (2018) 605–615.
[2] H. Kamran Haghighi, M. Irannajad, A. Fortuny, A.M. Sastre, Recovery of germanium from leach solutions of fly ash using solvent extraction with various extractants, Hydrometallurgy 175 (2018) 164–169.
[3] A.E. Torma, H. Jiang, Extraction processes for gallium and germanium, Miner. Process. Extr. Metall. Rev. 7 (1991) 235–258.
[4] R. Höll, M. Kling, E. Schroll, Metallogenesis of germanium—a review, Ore Geol. Rev. 30 (2007) 145–180.
[5] R.R. Moskalyk, Review of germanium processing worldwide, Miner. Eng. 17 (2004) 393–402.
[6] L. Zhang, W. Guo, J. Peng, J. Li, G. Lin, X. Yu, Comparison of ultrasonic-assisted and regular leaching of germanium from by-product of zinc metallurgy, Ultrason. Sonochem. 31 (2016) 143–149.
[7] L. Zhang, Z. Xu, An environmentally-friendly vacuum reduction metallurgical process to recover germanium from coal fly ash, J. Hazard. Mater. 312 (2016) 28–36.
[8] S. Virolainen, J. Heinonen, E. Paatero, Selective recovery of germanium with N-methylglucamine functional resin from sulfate solutions, Sep. Purif. Technol. 104 (2013) 193–199.
[9] Mineral Commodity Summaries 2018: U.S. Geological Survey. Reston, Virginia, 2018.
[10] B. Robertz, J. Verhelle, M. Schurmans, The primary and secondary production of germanium: a life-cycle assessment of different process alternatives, JOM 67 (2015) 412–424.
[11] E. Güler, A. Seyrankaya, Precipitation of impurity ions from zinc leach solutions with high iron contents – a special emphasis on cobalt precipitation, Hydrometallurgy 164 (2016) 118–124.
[12] H. Han, W. Sun, Y. Hu, H. Tang, The application of zinc calcine as a neutralizing agent for the goethite process in zinc hydrometallurgy, Hydrometallurgy 147–148 (2014) 120–126.
[13] J. Han, C. Yang, X. Zhou, W. Gui, Dynamic multi-objective optimization arising in iron precipitation of zinc hydrometallurgy, Hydrometallurgy 173 (2017) 134–148.
[14] L.R. Bernstein, Germanium geochemistry and mineralogy, Geochim. Cosmochim. Acta 49 (1985) 2409–2422.
[15] N. Mondillo, G. Arfè, R. Herrington, M. Boni, C. Wilkinson, A. Mormone, Germanium enrichment in supergene settings: evidence from the Cristal nonsulfide Zn prospect, Bongará district, northern Peru, Miner. Depos. 53 (2018) 155–169.
[16] A. Di Maria, K. Van Acker, Turning industrial residues into resources: an environmental impact assessment of goethite valorization, Engineering 4 (2018) 421–429.
[17] M. Pelino, C. Cantalini, C. Abbruzzese, P. Plescia, Treatment and recycling of goethite waste arising from the hydrometallurgy of zinc, Hydrometallurgy 40 (1996) 25–35.
[18] L. Zhang, Z. Xu, A critical review of material flow, recycling technologies, challenges and future strategy for scattered metals from minerals to wastes, J. Clean. Prod. 202 (2018) 1001–1025.
[19] A.K. Pabby, A.M. Sastre, Solvent extraction: principles and practices, Reference Module in Chemistry, Molecular Sciences and Chemical Engineering, Elsevier, 2018.
[20] E. Quijada-Maldonado, M.J. Torres, J. Romero, Solvent extraction of molybdenum (VI) from aqueous solution using ionic liquids as diluents, Sep. Purif. Technol. 177 (2017) 200–206.
[21] A. Berthod, M.J. Ruiz-Ángel, S. Carda-Broch, Recent advances on ionic liquid uses in separation techniques, J. Chromatogr. A 1559 (2018) 2–16.
[22] D. Parmentier, S. Paradis, S.J. Metz, S.K. Wiedmer, M.C. Kroon, Continuous process for selective metal extraction with an ionic liquid, Chem. Eng. Res. Des. 109 (2016) 553–560.
[23] C. Araneda, C. Fonseca, J. Sapag, C. Basualto, M. Yazdani-Pedram, K. Kondo,

E. Kamio, F. Valenzuela, Removal of metal ions from aqueous solutions by sorption onto microcapsules prepared by copolymerization of ethylene glycol dimethacrylate with styrene, Sep. Purif. Technol. 63 (2008) 517–523.
[24] A. Stojanovic, C. Morgenbesser, D. Kogelnig, R. Krachler, B.K. Keppler, Quaternary ammonium and phosphonium ionic liquids in chemical and environmental engineering, in: A. Kokorin (Ed.), Ionic Liquids: Theory, Properties, New Approaches, InTech, 2011, pp. 657–680.
[25] B. Wassink, D. Dreisinger, J. Howard, Solvent extraction separation of zinc and cadmium from nickel and cobalt using Aliquat 336, a strong base anion exchanger, in the chloride and thiocyanate forms, Hydrometallurgy 57 (2000) 235–252.
[26] C.P. Vibhute, S.M. Khopkar, Solvent extraction separation of germanium with Aliquat 336S from citric acid solutions, Bull. Chem. Soc. Jpn. 59 (1986) 3229–3232.
[27] S.K. Sahoo, Reversed phase extraction chromatographic separation of germanium with Aliquat 336S from citric acid, Bull. Chem. Soc. Jpn. 64 (1991) 2484–2487.
[28] Y.V. Yi, S.M. Khopkar, Reversed-phase column extractive separation of germanium with bis(2-ethylhexyl)phosphoric acid, Anal. Chim. Acta 221 (1989) 183–187.
[29] X.H. Ma, W.Q. Qin, X.-L. Wu, Extraction of germanium(IV) from acid leaching solution with mixtures of P204 and TBP, J. Cent. South Univ. 20 (2013) 1978–1984.
[30] E.G. Rochow, E.W. Abel, The chemistry of germanium, tin and lead, Pergamon Texts in Inorganic Chemistry, vol. 4, Pergamon, 1973, pp. 1–41.
[31] S. Nikitenko, A.M. Beale, A.M.J. van der Eerden, S.D.M. Jacques, O. Leynaud, M.G. O'Brien, D. Detollenaere, R. Kaptein, B.M. Weckhuysen, W. Bras, Implementation of a combined SAXS/WAXS/QEXAFS set-up for time-resolved in situ experiments, J. Synchrotron Rad. 15 (2008) 632–640.
[32] K.V. Klementev, Package "VIPER (visual processing in EXAFS researches) for windows", Nucl. Instrum. Methods Phys. Res., Sect. A 448 (2000) 299–301.
[33] M. Newville, EXAFS analysis using FEFF and FEFFIT, J. Synchrotron Rad. 8 (2001) 96–100.
[34] S. Bao, Y. Tang, Y. Zhang, L. Liang, Recovery and separation of metal ions from aqueous solutions by solvent-impregnated resins, Chem. Eng. Technol. 39 (2016) 1377–1392.
[35] Rohm and Haas Company, Amberlite XAD-16 Product Data Sheet, Philadelphia, USA, 2003.
[36] M. Halpern, What is Aliquat 336 and Adogen 464 HF? Let's clear up the confusion, PTC Organics Inc., 2012.
[37] S. Brunauer, L.S. Deming, W.E. Deming, E. Teller, On a theory of the van der Waals adsorption of gases, J. Am. Chem. Soc. 62 (1940) 1723–1732.
[38] J. Lemus, J. Palomar, M.A. Gilarranz, J.J. Rodriguez, Characterization of Supported Ionic Liquid Phase (SILP) materials prepared from different supports, Adsorption 17 (2011) 561–571.
[39] Y. Litaiem, M. Dhahbi, Measurements and correlations of viscosity, conductivity and density of an hydrophobic ionic liquid (Aliquat 336) mixtures with a non-associated dipolar aprotic solvent (DMC), J. Mol. Liq. 169 (2012) 54–62.
[40] R. Chandra, N.K. Dubey, V. Kumar, Phytoremediation of Environmental Pollutants, CRC Press, 2017.
[41] V.I. Parvulescu, E. Kemnitz, New Materials for Catalytic Applications, Elsevier Science, 2016.
[42] E.E. Martsinko, L.K. Minacheva, A.G. Pesaroglo, I.I. Seifullina, A.V. Churakov, V.S. Sergienko, Bis(citrato)germanates of bivalent 3d metals (Fe Co, Ni, Cu, Zn): Crystal and molecular structure of $[Fe(H_2O)_6][Ge(HCit)_2]\cdot 4H_2O$, Russ. J. Inorg. Chem. 56 (2011) 1243.
[43] V.S. Sergienko, L.K. Minacheva, A.V. Churakov, Specific features of the structure of germanium(IV) complexes with polybasic acids, Russ. J. Inorg. Chem. 55 (2010) 2001–2030.
[44] C. Sterling, Crystalline structure of germanomandelic acid, J. Inorg. Nucl. Chem. 29 (1967) 1211–1215.
[45] V.V. Negrebetsky, E.P. Kramarova, D.E. Arkhipov, A.A. Korlyukov, A.G. Shipov, Y.I. Baukov, Synthesis, structure, and stereochemical non-rigidity of bis[(2,2-dimethyl-4-oxo-2H-benzo[e][1,3]oxazin-3(4H)-yl)methyl] dichlorosilane and -germane, Russ. Chem. Bull. 64 (2015) 1808–1813.
[46] G.S. Pokrovski, J. Schott, Experimental study of the complexation of silicon and germanium with aqueous organic species: implications for germanium and silicon transport and Ge/Si ratio in natural waters, Geochim. Cosmochim. Acta 62 (1998) 3413–3428.
[47] D. Dupont, D. Depuydt, K. Binnemans, Overview of the effect of salts on biphasic ionic liquid/water solvent extraction systems: anion exchange, mutual solubility, and thermomorphic properties, J. Phys. Chem. B 119 (2015) 6747–6757.
[48] W. Weber, G.W. Gokel, Phase Transfer Catalysis in Organic Synthesis, first ed., Springer-Verlag, Berlin Heidelberg, 1977, p. 282.
[49] M.M. Shehata, Radiochemical studies relevant to cyclotron production of the radionuclides ^{71,72}As, ^{68}Ge/^{68}Ga and ^{76,77,80m}Br, PhD thesis Universität zu Köln, 2011.
[50] A. Manzak, O. Tutkun, Extraction of citric acid through an emulsion liquid membrane containing Aliquat 336 as carrier, Sep. Sci. Technol. 39 (2005) 2497–2512.
[51] A. Swarnkar, A. Keshav, A.K. Das, A.B. Soni, Modeling of the recovery of citric acid using Aliquat 336 in natural diluents, Int. J. Sci. Eng. Res. 2 (2014) 18–23.
[52] G.D. Redden, J. Li, J. Leckie, Chapter 13 - adsorption of U^{VI} and citric acid on goethite, gibbsite, and kaolinite: comparing results for binary and ternary systems, in: E.A. Jenne (Ed.), Adsorption of Metals by Geomedia, Academic Press, San Diego, 1998, pp. 291–315.
[53] C. García-Balboa, I.C. Bedoya, F. González, M.L. Blázquez, J.A. Muñoz, A. Ballester, Bio-reduction of Fe(III) ores using three pure strains of Aeromonas hydrophila, Serratia fonticola and Clostridium celerecrescens and a natural consortium, Bioresour. Technol. 101 (2010) 7864–7871.